Sleight, R., & Kent, C. (1983b) *J. Biol. Chem. 258*, 836–839.
Sleight, R., & Dao, H. T. (1990) *Lipids 25*, 100–107.
Vance, D. E. (1989) in *Phosphatidylcholine Metabolism* (Vance, D. E., Ed.) pp 36–43, CRC Press, Boca Raton, FL.
Weinhold, P. A., Rounsifer, M. E., & Feldman, D. A. (1986) *J. Biol. Chem. 261*, 5104–5110.
Weinstein, J. N., Klausner, R. D., Innerarity, T., Ralston, E., & Blumenthal, K. (1981) *Biochim. Biophys. Acta 647*, 270–284.
Wetterau, J. R., & Jonas, A. (1982) *J. Biol. Chem. 257*, 10961–10966.
Wickner, W. T. (1977) *Biochemistry 16*, 254–258.
Yao, Z., Jamil, H., & Vance, D. E. (1990) *J. Biol. Chem. 265*, 4326–4331.

Cholesterol Esterase Catalyzed Hydrolysis of Mixed Micellar Thiophosphatidylcholines: A Possible Charge-Relay Mechanism†

Larry D. Sutton,‡ Stacey Froelich,‡ H. Stewart Hendrickson,§ and Daniel M. Quinn*,‡

Department of Chemistry, The University of Iowa, Iowa City, Iowa 52242, and Department of Chemistry, St. Olaf College, Northfield, Minnesota 55057

Received August 20, 1990; Revised Manuscript Received March 21, 1991

ABSTRACT: Mechanistic features of cholesterol esterase catalyzed hydrolysis of two thiophospholipids, *rac*-1-(hexanoylthio)-2-hexanoyl-3-glycerophosphorylcholine (6TPC) and *rac*-1-(decanoylthio)-2-decanoyl-3-glycerophosphorylcholine (10TPC), have been characterized. The hydrolysis of 10TPC that is contained in mixed micelles with Triton X-100 occurs strictly at the micellar interface, since the reaction rate is independent of the micelle concentration but depends hyperbolically on the mole fraction of the substrate in the micelles. This latter observation allows one to calculate the interfacial kinetic parameters V^*_{max} and K^*_m. The hydrolyses of 10TPC and *p*-nitrophenyl butyrate are similarly inhibited by the transition state analogue inhibitor phenyl-*n*-butylborinic acid, and therefore, physiological and nonphysiological substrates are processed at the same active site. The similarity of k^*_{cat} values for the acyl-similar substrates 10TPC and *p*-nitrophenyl decanoate indicates that the phospholipase A_1 activity of cholesterol esterase is partially rate limited by turnover of a decanoyl-enzyme intermediate. Solvent isotope effects on V^*_{max} and V^*_{max}/K^*_m (which monitors acylation only) are ~2–3 and are consistent with transition states that are stabilized by general acid–base proton transfers. Proton inventories of V^*_{max}/K^*_m indicate that simultaneous proton transfers stabilize the acylation transition state, which requires a multifunctional acid–base machinery (perhaps a charge–relay system) in the cholesterol esterase active site. Similar results are obtained for the 6TPC reaction, both in the presence and absence of Triton X-100 micelles.

Pancreatic cholesterol esterase (CEase)[1] is a digestive lipolytic enzyme that is secreted into the duodenum in response to a dietary fat load. CEase is a rather promiscuous catalyst. In the intestinal lumen the enzyme catalyzes the hydrolysis of such diverse esters as triacylglycerols, cholesteryl esters, and phospholipids (Brockerhoff & Jensen, 1974; Kritchevsky & Kothari, 1978; Rudd & Brockman, 1984), with consequent release of amphipathic molecules that can be taken up by the cells of the intestinal mucosa. Accordingly, CEase activity is necessary for the full absorption of dietary fats (Bhat & Brockman, 1982; Gallo et al., 1984). In vitro CEase activity is increased by interaction with bile salts, which are physiological activators of the enzyme (Brockerhoff & Jensen, 1974; Kritchevsky & Kothari, 1978; Rudd & Brockman, 1984).

CEase catalyzes ester turnover via an acylenzyme mechanism (Stout et al., 1985; Lombardo & Guy, 1981) that is reminiscent of the mechanism of serine protease catalysis (Stroud, 1974; Blow, 1976; Kraut, 1977; Polgar, 1987). The best defined CEase reactions, in a mechanistic sense, are those for turnover of lipid *p*-nitrophenyl esters (Sutton et al., 1990; Sutton & Quinn, 1990). Proton inventory experiments (Schowen, 1978; Schowen & Schowen, 1982) with these substrates invariably indicate that chemical transition states are stabilized by simple general acid–base (i.e., one-proton) catalysis. However, recent sequence comparisons among CEase (Kissel et al., 1989), AChE (Schumacher et al., 1986), and BuChE (Lockridge et al., 1987a) suggest that the three enzymes may contain active site catalytic triads like those of the serine proteases. Scheme I compares three subsequences of CEase and the cholinesterases that contain (in the CEase sequence) S194, H435, and D79. Since the corresponding serine residues of the cholinesterases are the active site nucleophiles, the inescapable conclusion is that S194 plays this

† This work was supported by NIH Grant HL30089. D.M.Q. was a recipient of a Research Career Development Award (HL01583, 1985–90).

* To whom correspondence should be addressed.
‡ The University of Iowa.
§ St. Olaf College.

[1] Abbreviations: 6TPC, *rac*-1-(hexanoylthio)-2-hexanoyl-3-glycerophosphorylcholine; 10TPC, *rac*-1-(decanoylthio)-2-decanoyl-3-glycerophosphorylcholine; CEase, cholesterol esterase; BuChE, butyrylcholinesterase; AChE, acetylcholinesterase; V^*_{max}, interfacial $V_{max} = k^*_{cat}[E]_T$; K^*_m, interfacial K_m; TX100, Triton X-100; DTNB, 5,5′-dithiobis(2-nitrobenzoic acid); $^{D_2O}V^*_{max} = (V^*_{max})^{H_2O}/(V^*_{max})^{D_2O}$, solvent isotope effect on V^*_{max}; $^{D_2O}V^*_{max}/K^*_m$, corresponding solvent isotope effect on V^*_{max}/K^*_m; V_i, initial velocity; X_S, mole fraction of substrate in mixed micelles; PLA_1, phospholipase A_1; PLA_2, phospholipase A_2; PBBA, phenyl-*n*-butylborinic acid; MeCN, acetonitrile; NaTC, sodium taurocholate. Single-letter amino acid codes used are C, cysteine; D, aspartate; H, histidine; and S, serine.

0006-2960/91/0430-5888$02.50/0

Scheme I: Sequence Comparison of CEase and Cholinesterases

Active Site Sequences

CEase	I-T-I-F-G-E-S^{194}-A-G-A-A-S-V
AChE	V-T-I-F-G-E-S^{200}-A-G-G-A-S-V
BuChE	V-T-L-F-G-E-S^{198}-A-G-A-A-S-V

Sequences Containing Glu/Asp

CEase	E^{78}-D^{79}-C-L-Y-L-N-I-W-V-P
AChE	E^{92}-D^{93}-C-L-Y-L-N-I-W-V-P
BuChE	E^{90}-D^{91}-C-L-Y-L-N-V-W-I-P

Sequences Containing His

CEase	W-M-G-A-D-H^{435}-A-D-D-L-Q-Y-V-F-G-K-P
AChE	W-M-G-V-I-H^{440}-G-Y-E-I-E-F-V-F-G-L-P
BuChE	W-M-G-V-M-H^{438}-G-Y-E-I-E-F-V-F-G-L-P

role in CEase catalysis. This conclusion is supported by experiments by DiPersio et al. (1990), who showed by site-directed mutagenesis and radiolabeling with [^{3}H]diisopropyl fluorophosphate that S194 is required for rat pancreatic CEase activity. The region of CEase that contains residues 159–221 has high sequence similarity with the cholinesterases (~70%). Outside this region sequence similarity is minimal, save the short sequences around H435 and D79 outlined in Scheme I. DiPersio et al. (1991) have also found by site-directed mutagenesis of rat pancreatic CEase that H435, but not H420, is required for activity. Of the three intrasubunit disulfide bonds in AChE (MacPhee-Quigley et al., 1986) and BuChE (Lockridge et al., 1987b), there are two whose contributing cysteines are matched by cysteines C64, C80, C247, and C258 in the CEase sequence, and therefore, the folding patterns of the three enzymes must be similar. A constituent of one of the disulfide bonds (C80, C92, and C94 in CEase, BuChE, and AChE, respectively) is adjacent to the aspartate of the putative charge–relay system. These comparisons suggest that the enzymes are evolutionarily related and lead one to suspect that there must be mechanistic relatedness among the enzymes as well. This latter conclusion is certainly not supported by a superficial functional comparison: CEase catalyzes the interfacial hydrolysis of lipid esters that are contained in supramolecular aggregates, while the cholinesterases catalyze the turnover of low molecular weight choline esters in homogeneous solution.

In this paper the CEase-catalyzed hydrolysis of thiophospholipids that are contained in mixed micelles with TX100 is described. This system is a good deal more biomimetic than the well-characterized lipid *p*-nitrophenyl esters (Sutton et al., 1990; Sutton & Quinn, 1990). The interfacial nature and prototropic catalysis of the phospholipolysis reaction are characterized herein. In particular, the possibility that CEase acts as a multiproton, perchance charge–relay, catalyst is probed. As we shall see, there is a functional difference in the way that CEase stabilizes chemical transition states of nonphysiological and physiological reactions.

Experimental Procedures

Materials. Porcine pancreatic CEase (EC 3.1.1.13) was isolated by a modification (Sutton et al., 1990) of the procedure of Rudd et al. (1987). Fresh porcine pancreas was purchased from a local slaughterhouse and was frozen with dry ice immediately upon removal from the animals. The purified enzyme was stored at −70 °C in 0.1 M sodium phosphate buffer, pH 7.0, that contained 0.1 N NaCl, 3 mM NaTC, 2 mM benzamidine hydrochloride, and 0.2 mM *N*-benzoylarginine.

The thiophospholipid substrates 6TPC and 10TPC were synthesized as described by Hendrickson et al. (1983). TX100, NaTC, and DTNB were purchased from Sigma Chemical Co. Deuterium oxide (99.8% D) was purchased from Sigma Chemical Co. and Aldrich Chemical Co. Distilled protium oxide was deionized by passage through a Barnstead mixed-bed ion-exchange column (Sybron Corp.). HPLC grade acetonitrile and chloroform were purchased from Fisher Scientific. All salts used in buffer preparations were commercially available reagent grade products. All materials were used as received.

Kinetic Measurements and Data Reduction. Reactions were followed by monitoring the release of the free thiol product by coupling with DTNB. The absorbance at 412 nm of the 5-thio-2-nitrobenzoic acid chromophore was measured as a function of time on one of the following systems: a Beckman DU-40 UV–visible spectrophotometer, interfaced to an IBM PC; a Hewlett-Packard HP8452 diode-array UV–visible spectrophotometer, interfaced to an IBM PC-AT. CEase-catalyzed hydrolysis of *p*-nitrophenyl butyrate (PNPB) was followed at 400 nm on an automated enzyme kinetics system that consists of a ZymateI robot (Zymark Corp., Hopkinton, Mass.), a Beckman DU-7 UV–visible spectrophotometer, and assorted peripherals (Quinn et al., 1988). Reactions were thermostated by circulating water from refrigerated water baths through the jacketed cell holders of the spectrophotometers. Equivalent buffers, those that contain the same concentrations of all solutes (Schowen, 1978; Schowen & Schowen, 1982), were prepared in H_2O and D_2O for solvent isotope effect and proton inventory experiments.

Initial rates were calculated by linear least-squares analysis of time courses that correspond to ≤5% of total substrate turnover. Mixed micelles were prepared by the following procedure: (a) an appropriate volume of a stock solution of 10TPC in $CHCl_3$ was added to a glass vial; (b) the organic solvent was evaporated; (c) the necessary amount of TX100 was added to the lipid film and the components were thoroughly mixed; (d) the mixture was slowly dissolved, with stirring, in the reaction buffer. TX100 concentrations of such preparations were always well above the critical micelle concentration of 0.2–0.3 mM (Burdette & Quinn, 1986). The interfacial kinetic parameters K_m^* and V_{max}^* for 10TPC turnover were determined in the following way: (a) the mole fraction of thio-PC substrate in mixed micelles with TX100 was varied at constant [DTNB] (e.g., 1 mM) and constant concentration of micelle components (e.g., 2.5 mM), and corresponding initial velocities were measured; (b) $\{V_i, X_S\}$ data were fit to the following interfacial catalysis version of the Michaelis–Menten equation by nonlinear least-squares procedures (Wentworth, 1965)

$$V_i = \frac{V_{max}^* X_S}{K_m^* + X_S} \quad (1)$$

In eq 1, V_i is the initial velocity, X_S is the mole fraction of substrate in the mixed micelles, and K_m^* and V_{max}^* are defined in Results. The pseudo-first-order rate constant V_{max}^*/K_m^* was also determined by fitting time course data over at least three half-lives of reaction to the following equation by nonlinear least-squares procedures (Wentworth, 1965)

$$A_t = (A_0 - A_\infty)e^{-kt} + A_\infty \quad (2)$$

In this equation, A_t, A_0, and A_∞ are the absorbances at times t, 0, and ∞, respectively, and $k = V_{max}^*/K_m^*$. For these reactions, initial substrate mole fractions < $K_m^*/10$ were used.

Inhibition of CEase by phenyl-*n*-butylborinic acid (PBBA) was characterized as described by Sutton et al. (1986).

Scheme II: CEase Substrates

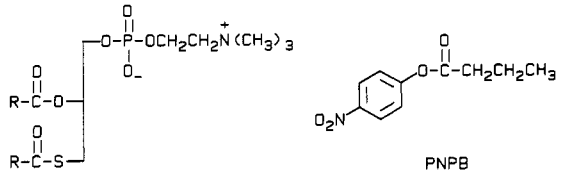

R = C_5H_{11}, 6TPC

R = C_9H_{19}, 10TPC

Proton Inventories. Measurements of the rate or rate constant of a reaction in a series of equivalent mixtures of H_2O and D_2O comprises a "proton inventory" that, with certain limitations, can be used to determine the number and nature of prototropic catalytic elements (e.g., proton transfers) that contribute to the solvent isotope effect (Schowen, 1978; Schowen & Schowen, 1982). The general expression for the dependence of the rate constant k_n on the atom fraction n of deuterium in mixed isotopic buffers is the Gross–Butler equation

$$k_n = k_0 \frac{\prod_i (1 - n + n\phi_i^T)}{\prod_j (1 - n + n\phi_j^R)} \quad (3)$$

The numerator and denominator respectively contain products of terms for contributions to the solvent isotope effect ^{D_2O}k by transition-state protons (i.e., ϕ_i^T) and reactant-state protons (i.e., ϕ_j^R). Only those protons contribute that have fractionation factors $\phi \neq 1$, and since the common amino acid side chains that are involved in prototropic and/or nucleophilic catalysis have $\phi^R = 1$ (Schowen, 1978; Schowen & Schowen, 1982),[2] eq 3 reduces to a polynomial function of n

$$k_n = k_0 \prod_i (1 - n + n\phi_i^T) \quad (4)$$

Therefore, one can use polynomial regression analysis (Schowen, 1978) to evaluate the significances of linear, quadratic, cubic, etc. descriptions of the dependence of k_n on n. In our laboratory the microcomputer program MYSTAT, available from SYSTAT (1800 Sherman Ave., Evanston, IL 60201), is used for polynomial regressions, and outputted percent confidence levels are used to select the appropriate polynomial description of the proton inventory. When only the linear description is indicated (i.e., one proton transfer stabilizes the transition state), the fractionation factor ϕ^T is calculated by linear least-squares analysis. When a quadratic dependence is indicated, the proton inventory is fit by nonlinear least-squares methods (Wentworth, 1965) to eq 5 ($\phi_1^T = \phi_2^T$) or to eq 6 ($\phi_1^T \neq \phi_2^T$). The ϕ^T values calculated from least-

$$k_n = k_0(1 - n + n\phi_1^T)^2 \quad (5)$$

$$k_n = k_0(1 - n + n\phi_1^T)(1 - n + n\phi_2^T) \quad (6)$$

squares analyses of proton inventories are just reciprocals of the contributions of the respective transition-state protons to the solvent isotope effect. The theory and application of the proton inventory technique to enzyme reactions have been thoroughly described (Schowen, 1978; Schowen & Schowen, 1982).

Results

DTNB Coupling. Scheme II shows the structures of the substrates used in this study. In order to utilize DTNB as a colorimetric indicator in the coupled CEase phospholipolysis assay, it was first necessary to demonstrate that DTNB has no effect on the kinetics. The effect of DTNB was characterized by following the rate of CEase-catalyzed hydrolysis of the well-characterized substrate PNPB (Stout et al., 1985). Figure 1 shows that as much as 1 mM DTNB has no effect on the PNPB reaction. Therefore, DTNB does not effect substrate binding or catalytic turnover at the CEase active site. Figure 1 also shows that there is little change in the rate of CEase-catalyzed hydrolysis of 10TPC for DTNB concentrations up to 1 mM. These results demonstrate that CEase kinetics are not rate limited by the redox coupling of the product and indicator, and hence the rates are only those of CEase-catalyzed turnover of 10TPC.

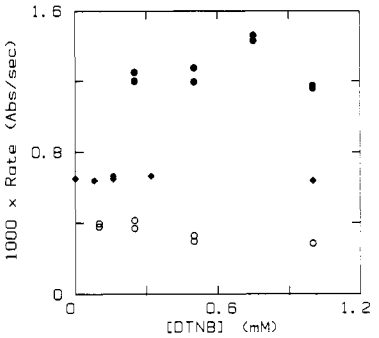

FIGURE 1: Effect of DTNB on CEase catalysis. Diamonds show the effect of DTNB on initial rates of CEase-catalyzed hydrolysis of PNPB. Reactions were monitored at 25.25 ± 0.05 °C in 0.1 M sodium phosphate buffer, pH 7.04, that contained 0.1 N NaCl, 1 mM TX100, 0.2 mM PNPB, 26 ng mL^{-1} CEase, and 2.5% (v/v) MeCN. Closed and open circles show the effect of varying DTNB concentration on the rate of CEase-catalyzed hydrolysis of 10TPC in buffered H_2O and D_2O, respectively. Rates plotted as closed circles were measured at 25.08 ± 0.05 °C in 0.1 M sodium phosphate buffer, pH 7.04, that contained 0.1 N NaCl, 2 mM TX100, 0.5 mM 10TPC, 15 μM NaTC, and 32 μg mL^{-1} CEase. These rates were divided by 2 to make the scales of the three data sets comparable. Rates plotted as open circles were measured at 25.15 ± 0.09 °C in 0.1 M sodium phosphate buffer, pD 7.55, that contained 0.1 N NaCl, 2 mM TX100, 0.5 mM 10TPC, 1.5 μM NaTC, and 1 μg mL^{-1} CEase.

10TPC Kinetics. Since 10TPC is not very water-soluble, catalysis should only occur at the mixed micelle–water interface. The mechanism for a single-substrate lipolytic enzyme reaction has been described previously (Brockman, 1984; Verger & DeHaas, 1976). A steady-state derivation for this mechanism yields the following equation for the initial velocity of the reaction

$$V_i = \frac{V^*_{max} X_S [I_S]}{X_S [I_S] + K^*_m [I_S] + K_D K^*_m} \quad (7)$$

The equation is pro forma that for an equilibrium, ordered two-substrate enzyme reaction (Cleland, 1977), but with the following differences. (a) The enzyme first binds to the substrate-containing interface I_S. CEase is increasingly interface-bound as the micelle concentration (and hence interface area) is increased. Since the micelles contain a certain substrate mole fraction X_S, the micelle concentration is proportional to the bulk substrate concentration (i.e., substrate concentration in molar units). (b) Once micelle-bound, the CEase active site binds substrate in the interface. The mole fraction of substrate among total micelle components provides a convenient measure of interfacial substrate concentration, and hence K^*_m is in units of mole fraction. In the general case, one must vary X_S at several fixed values of $[I_S]$ in order to determine the constants V^*_{max} ($=k^*_{cat}[E]_T$), K^*_m [$=(k_2 + k^*_{cat})/k_1$, where k_1 and k_2 are the respective rate constants for

[2] The thiol group of cysteine, which has $\phi = 0.4$–0.6, is an exception (Schowen, 1978; Schowen & Schowen, 1982).

Table I: Solvent Isotope Effects for CEase-Catalyzed Hydrolysis of 6TPC and 10TPC

substrate	[TX100] (mM)	[NaTC] (μM)	$^{D_2O}V^*_{max}$	$^{D_2O}V^*_{max}/K^*_m$	ϕ_1^T	ϕ_2^T
6TPC	0.04	0.12	3.51 ± 0.09[a]	1.4 ± 0.1[a]		
	0.04	3		1.8 ± 0.1[b]	0.75 ± 0.01[c]	0.75 ± 0.01[c]
	1	0.12	1.9 ± 0.3[a]	1.7 ± 0.5[a]		
	1	3		2.7 ± 0.1[b]	0.41 ± 0.03[c]	0.88 ± 0.06[c]
10TPC	2.5	15	2.3 ± 0.1[a]	2.1 ± 0.1[a]		
	2.5	240		3.2 ± 0.3[b]	0.56 ± 0.01[c]	0.56 ± 0.01[c]

[a] Values were determined by fitting initial velocities to the Michaelis–Menten equation for 6TPC or to the interfacial version of the Michaelis–Menten equation (eq 1 under Experimental Procedures) for 10TPC. Error limits are standard errors of the least-squares parameters. [b] Rate constants were determined by first-order kinetics. Isotope effects are means of triplicate determinations. Error limits are standard errors of the means. [c] Fractionation factors for 10TPC and for 6TPC in the absence of TX100 micelles were calculated by fitting proton inventories to eq 5 under Experimental Procedures, and those for 6TPC in the presence of TX100 micelles were calculated by fitting data to eq 6. Error limits are standard errors of the least-squares parameters.

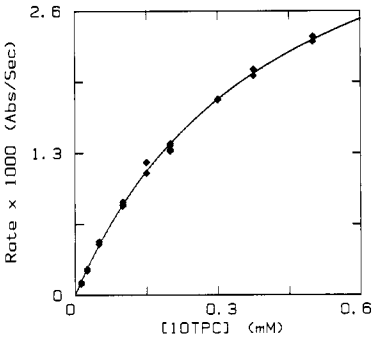

FIGURE 2: Dependence of initial rate on X_S for CEase-catalyzed hydrolysis of 10TPC. Reaction conditions were the same as those in the legend of Figure 1 (closed circles in Figure 1), save that the mol % of 10TPC in mixed TX100 micelles was varied and the DTNB concentration was 1 mM. The solid line is a nonlinear least-squares fit of the data to eq 1 under Experimental Procedures.

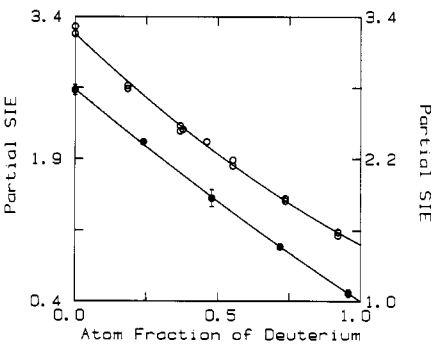

FIGURE 3: Proton inventories for V^*_{max}/K^*_m of CEase-catalyzed hydrolysis of 10TPC (○, left y-axis) and 6TPC (●, right y-axis). Rate constants were calculated by fitting time course data to eq 2 under Experimental Procedures. Reactions were run at pH 7.00 in H_2O, pD 7.56 in D_2O, and at equivalent pL (L = H or D) in mixed H_2O–D_2O buffers (Schowen, 1978; Schowen & Schowen, 1982). 10TPC reactions were monitored at 24.95 ± 0.05 °C in 0.1 M sodium phosphate buffer that contained 0.1 N NaCl, 1 mM DTNB, 0.51 mg mL^{-1} CEase, 2.5 mM TX100, 240 μM NaTC,and 0.015 mM 10TPC. The individual rate constants are plotted. The solid line is a nonlinear least-squares fit to eq 5 under Experimental Procedures. 6TPC reactions were monitored at 25.1 ± 0.1 °C in 0.1 M sodium phosphate buffer that contained 0.1 N NaCl, 1 mM DTNB, 1 mM TX100, 0.06 mM 6TPC, 3 μM NaTC, and 3.2 μg mL^{-1} CEase. Plotted points are means ± standard errors of four to seven observations at each atom fraction of deuterium. The solid line is a nonlinear least-squares fit to eq 6 of Experimental Procedures.

formation and dissociation of the interfacial Michaelis complex], and K_D, the enzyme–micelle dissociation constant (Hendrickson & Dennis, 1984).

The initial rate of CEase-catalyzed hydrolysis of 10TPC was found to be independent of the total mixed micelle concentration. This indicates that $[I_S] \gg K_D$, and therefore eq 7 simplifies to eq 1 under Experimental Procedures. In addition, a linear dependence of rate on enzyme concentration was observed, as expected if the Michaelis–Menten equation, albeit in interfacial terms, describes these kinetics, since $V^*_{max} = k^*_{cat}[E]_T$.

Figure 2 shows the dependence of initial rate on X_S for CEase-catalyzed hydrolysis of 10TPC. For this experiment, in which total micelle concentration was 2.5 mM, K^*_m = 16 ± 4 mol % and V^*_{max} = 0.29 ± 0.02 μM s^{-1}. When the total micelle concentration was 5 mM, K^*_m = 15 ± 1 mol % and V^*_{max} = 0.26 ± 0.01 μM s^{-1} (plot not shown). If substrate were reacting with CEase in the bulk phase (i.e., off the interface), then at higher total micelle concentrations the bulk phase concentration of the substrate should be doubled and the value of K^*_m should decrease. That it does not is firm evidence that the reaction occurs only at the micelle interface. By using a molecular mass for CEase of 80000, $k^*_{cat} = V^*_{max}/[E]_T$ = 0.8 ± 0.1 s^{-1}. This value of k^*_{cat} is similar to that for CEase-catalyzed turnover of the acyl-similar substrate p-nitrophenyl decanoate (k^*_{cat} = 1.5 s^{-1}).[3] The k^*_{cat}/K^*_m values for the reaction, determined by initial rates and continuous first-order assay, were 1800 ± 100 M^{-1} s^{-1} and 1100 ± 100 M^{-1} s^{-1}, respectively. The similarity of the values obviates the problem of product inhibition in the continuous assay. The continuous assay showed good adherence to first-order kinetics for four to five half-lives, which also indicates that product inhibition is not a complication.

Solvent deuterium kinetic isotope effects on V^*_{max} and V^*_{max}/K^*_m of CEase-catalyzed hydrolysis of 10TPC were measured by initial rates and continuous first-order kinetics and are gathered in Table I. The magnitudes of the isotope effects are consistent with prototropic stabilization of chemical transition states. The lack of a solvent isotope effect on K^*_m indicates that D_2O does not change the conformation or stability of CEase. The value $^{D_2O}V^*_{max}/K^*_m$ increases as the concentration of the bile salt taurocholate, a physiological effector of CEase (Brockerhoff & Jensen, 1974; Kritchevsky & Kothari, 1978; Rudd & Brockman, 1987), increases. This trend was observed in both the presence and absence of TX100 micelles when 6TPC was the substrate and therefore does not arise from an effect of taurocholate on the substrate-containing mixed micelles. Since the dissociation constant for interaction of taurocholate with porcine pancreatic CEase is 5–20 μM (Tsujita et al., 1987), increasing saturation of the bile salt binding site increases the solvent isotope effects for thiophospholipid turnover.

Proton inventories of the 10TPC reaction were determined by continuous first-order assays, and the nonlinear and downward bulging plot of one of these experiments is shown

[3] The k^*_{cat} for p-nitrophenyl decanoate turnover was determined as described by Sutton et al. (1990) and with the same CEase preparation used for characterizing 10TPC turnover.

in Figure 3. Polynomial regression analysis indicated that the proton inventory is described by a quadratic equation at >99.9% confidence. The results of least-squares analysis of proton inventories are also contained in Table I and indicate that two transition-state protons make equal contributions to the solvent isotope effect (i.e., $1/\phi^T = 1.79 \pm 0.03$).

6TPC Kinetics. Unlike the kinetics of 10TPC hydrolysis, CEase-catalyzed hydrolysis of 6TPC is not a strictly interfacial process. For example, the respective k_{cat} and K_m values at various TX100 concentrations are (number of determinations in parentheses) with 0.04 mM TX100, 160 ± 40 s^{-1}, 1.4 ± 0.6 mM (4); with 1 mM TX100, 260 ± 30 s^{-1}, 1.8 ± 0.4 mM (2); with 2 mM TX100, 259 ± 9 s^{-1}, 2.1 ± 0.1 mM (1); with 10 mM TX100, 157 ± 4 s^{-1}, 1.6 ± 0.1 mM (1); and with 20 mM TX100, 47 ± 1 s^{-1}, 1.4 ± 0.1 mM (1). These data show that K_m stays relatively constant. If the 6TPC reaction occurred exclusively at the interface, K_m^* in mole fraction units would be constant, and therefore, K_m in molar units would be a linear function of the TX100 concentration. The data also show that k_{cat} is little affected, save at the highest concentration, by increasing TX100. The fact that k_{cat} is ~200-fold greater than k_{cat}^* for CEase-catalyzed hydrolysis of 10TPC indicates that CEase is more specific for short-chain phosphatidylcholine substrates. A similar specificity trend was observed for turnover of lipid *p*-nitrophenyl esters by CEase (Sutton et al., 1990).

Solvent isotope effects on V_{max} and V_{max}/K_m of 6TPC turnover were measured by initial rates and first-order kinetics and are gathered in Table I. The isotope effects generally fall in the range 1.5–4, which again is consistent with rate determination of V_{max} and V_{max}/K_m by transition states that are stabilized by proton-transfer catalysis. Figure 3 shows the proton inventory of V_{max}/K_m of CEase-catalyzed hydrolysis of 6TPC in the presence of TX100 micelles. As the data in Table I show, the proton inventory is best described by a model in which two protons make unequal contributions to the solvent isotope effect (i.e., $1/\phi_1^T = 2.4 \pm 0.2$ and $1/\phi_2^T = 1.14 \pm 0.07$). The small contribution from the second proton could arise not from proton transfer but from a secondary isotope effect. The proton inventory in the absence of TX100 micelles was also curved (graph not shown), and the corresponding solvent isotope effect arises from equal contributions from two transition-state protons (cf. Table I).

Inhibition Studies. Phenyl-*n*-butylboronic acid (PBBA) is a potent competitive inhibitor of CEase-catalyzed hydrolysis of PNPB (Sutton et al., 1986). A single preparation of CEase was used to test PBBA as an inhibitor of both the PNPB and 10TPC reactions. The respective K_i values were 12 ± 1 and 7.5 ± 0.4 nM. Since the K_i values are similar, are both consonant with potent inhibition, and are both similar to the reported value for inhibition of CEase-catalyzed hydrolysis of PNPB in the absence of TX100 (Sutton et al., 1986), one can conclude that CEase-catalyzed hydrolyses of PNPB and 10TPC occur at a common active site.

Discussion

Physiological CEase catalysis provides a route, along with pancreatic lipase and PLA_2, for the digestion in the intestines of lipid ester substrates and consequent absorption of fatty acids, glycerides, and cholesterol. The work described herein initiates efforts to define the dynamics and structural courses (especially transition-state structures) of CEase reactions that bear resemblance to physiological catalysis. The substrates chosen for study of the PLA_1 activity of CEase, 6TPC, and 10TPC, provide several experimental advantages. (a) They are easily incorporated into mixed micelles with TX100 to give preparations that are optically clear. Presumably, this feature could also be exploited to prepare a yet more biomimetic mixed micelle with bile salts, which are physiological effectors of CEase catalysis (Brockerhoff & Jensen, 1974). (b) Reactions are easily and continuously monitored by coupled spectrophotometric assay with DTNB. (c) The CEase-catalyzed hydrolysis of 10TPC has the kinetic hallmarks of a reaction that occurs exclusively at the micelle surface. (d) 6TPC is sufficiently soluble so that both mixed micellar and nonmicellar reactions can be studied.

Scheme III: Cholesterol Esterase Mechanism

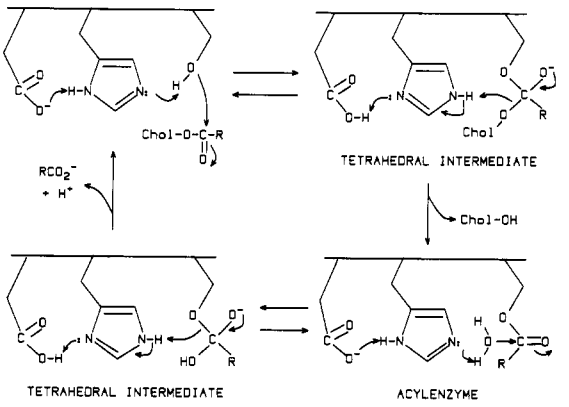

Scheme III outlines a proposed mechanism for CEase catalysis, and includes roles for S194, H435, and D79 of the conserved sequences shown in Scheme I. Since one need not be concerned with the on and off rate constants for interaction of CEase with the micelle surface, the kinetic parameters for the mechanism of Scheme III are analogous to those for a homogeneous phase acylenzyme mechanism.

$$k_{cat}^* = \frac{k_3 k_5}{k_3 + k_5} \tag{8}$$

$$k_{cat}^*/K_m^* = \frac{k_1 k_3}{k_2 + k_3} \tag{9}$$

Comparison of k_{cat}^* values for acyl-similar substrates allows one to gauge the contributions of acylation (k_3) and deacylation (k_5) to rate determination. Both the acylation and deacylation stages likely involve separate steps for formation and decomposition of tetrahedral intermediates, as shown in Scheme III. For lipid *p*-nitrophenyl ester substrates k_{cat}^* is rate limited by deacylation (Stout et al., 1985; Sutton et al., 1990). The fractional rate determination by deacylation is given by eq 10. From eq 8 one notices that the ratio of k_{cat}^* values for

$$f_d = \frac{k_3}{k_3 + k_5} \tag{10}$$

two acyl-similar substrates is the ratio of fractional rate determinations by deacylation as shown in eq 11. The k_{cat}^* values

$$k_{cat}^{*A}/k_{cat}^{*B} = \frac{k_3^A/(k_3^A + k_5)}{k_3^B/(k_3^B + k_5)} = f_d^A/f_d^B \tag{11}$$

for 10TPC and *p*-nitrophenyl decanoate, measured on the same day with the same preparation of CEase, were 0.8 s^{-1} and 1.5 s^{-1}, respectively, which is consistent with 56% rate determination by deacylation for the 10TPC reaction.

The parameter k_{cat}^*/K_m^*, on the other hand, monitors events in the acylation stage of catalysis only, as indicated by eq 9 (k_1 and k_2 are the rate constants for formation and dissociation, respectively, of the interfacial Michaelis complex E*S). The consistent observation of solvent isotope effects of 1.5–4 for

k^*_{cat} and k^*_{cat}/K^*_m of 10TPC and 6TPC reactions indicates that transition states of chemical steps are rate-limiting and are stabilized by proton transfers in both the acylation and deacylation stages of the PLA_1 activity of CEase. Moreover, since sizable solvent isotope effects for 6TPC turnover are observed when the substrate is in mixed TX100 micelles and when it is not, the micellar nature of CEase reactions does not introduce artifacts into isotope effect determinations. This assertion is supported by the observation that the proton inventories of k_{cat}/K_m for 6TPC turnover in the presence and absence of TX100 micelles are similar in shape.

A final point concerns the multiplicity of proton transfers for CEase-catalyzed reactions. For CEase-catalyzed hydrolysis of lipid *p*-nitrophenyl esters, both acylation and deacylation involve simple general acid–base, one-proton catalysis (Sutton et al., 1990). For the physiologically more relevant PLA_1 activity, a coupled proton transfer entity is elicited. For the substrate 10TPC, the proton inventory of k^*_{cat}/K^*_m is nonlinear (cf. Figure 3) and is interpreted in terms of equal contributions to the solvent isotope effect of 1.79 ± 0.03 from two transition-state proton transfers. For the shorter substrate 6TPC, the proton inventory is also nonlinear (cf. Figure 3), through the contributions to the solvent isotope effect from the two transition-state proton transfers are not necessarily equal. Apparently, when CEase catalyzes the hydrolysis of physiological substrates, the evolutionarily developed set of enzyme–substrate interactions that stabilizes the transition state includes concerted proton transfers. The observation of single proton catalysis of nonphysiological reactions but of multiple proton catalysis of biomimetic reactions has numerous precedents in the literature. Such observations have been made for reactions catalyzed by asparaginases (Quinn et al., 1980b) and various serine proteases, which include chymotrypsin (Stein & Strimpler, 1987), trypsin (Elrod et al., 1980), elastases (Stein & Strimpler, 1987; Stein et al., 1987), and α-lytic protease (Quinn et al., 1980a; Hunkapiller et al., 1976). As Schemes I and III suggest, a putative entity in CEase that could produce concerted transition-state proton transfers is a charge–relay system that consists of S194, H435, and D79, though a role for D79 in active site function has not yet been established. Moreover, since these amino acids are also contained in analogous subsequences of cholinesterases (Lockridge et al., 1987; Schumacher et al., 1986), one predicts that multiproton catalysis of cholinesterase-catalyzed reactions may also be observed. The list of enzymes that stabilize transition states via putative charge–relay catalysis has grown too long to blithely ignore. CEase represents the first enzyme that catalyzes heterogeneous biocatalytic processes to join this list.

References

Bhat, S. G., & Brockman, H. L. (1982) *Biochem. Biophys. Res. Commun. 109*, 486–492.

Blow, D. M. (1976) *Acc. Chem. Res. 9*, 145–152.

Brockerhoff, H., & Jensen, R. G. (1974) in *Lipolytic Enzymes*, pp 176–193, Academic Press, New York.

Brockman, H. L. (1984) in *Lipases* (Borgström, B., & Brockman, H. L., Eds.) pp 3–46, Elsevier, Amsterdam.

Burdette, R. A., & Quinn, D. M. (1986) *J. Biol. Chem. 261*, 12016–12021.

Cleland, W. W. (1977) *Adv. Enzymol. Relat. Areas Mol. Biol. 45*, 273–387.

DiPersio, L. P., Fontaine, R. N., & Hui, D. Y. (1990) *J. Biol. Chem. 265*, 16801–16806.

DiPersio, L. P., Fontaine, R. N., & Hui, D. Y. (1991) *J. Biol. Chem. 266*, 4033–4036.

Elrod, J. P., Hogg, J. L., Quinn, D. M., Venkatasubban, K. S., & Schowen, R. L. (1980) *J. Am. Chem. Soc. 102*, 3917–3922.

Gallo, L. L., Clark, S. B., Myers, S., & Vahouny, G. V. (1984) *J. Lipid Res. 25*, 604–612.

Hendrickson, H. S., & Dennis, E. A. (1984) *J. Biol. Chem. 259*, 5734–5739.

Hendrickson, H. S., Hendrickson, E. K., & Dybvig, R. H. (1983) *J. Lipid Res. 24*, 1532–1537.

Hunkapiller, M. W., Forgac, M. D., & Richards, J. H. (1976) *Biochemistry 15*, 5581–5588.

Kissel, J. A., Fontaine, R. N., Turck, C. W., Brockman, H. L., & Hui, D. Y. (1989) *Biochim. Biophys. Acta 1006*, 227–236.

Kraut, J. (1977) *Annu. Rev. Biochem. 46*, 331–358.

Kritchevsky, D., & Kothari, H. V. (1978) *Adv. Lipid Res. 16*, 221–226.

Lockridge, O., Bartels, C. F., Vaughan, T. A., Wong, C. K., Norton, S. E., & Johnson, L. L. (1987a) *J. Biol. Chem. 262*, 549–557.

Lockridge, O., Adkins, S., & LaDu, B. N. (1987b) *J. Biol. Chem. 262*, 12945–12952.

Lombardo, D., & Guy, O. (1981) *Biochim. Biophys. Acta 657*, 425–437.

MacPhee-Quigley, K., Vedvick, T. S., Taylor, P., & Taylor, S. S. (1986) *J. Biol. Chem. 261*, 13565–13570.

Polgar, L. (1987) in *Hydrolytic Enzymes* (Neuberger, A., & Brocklehurst, K., Eds.) pp 159–200, Elsevier, Amsterdam.

Quinn, D. M., Elrod, J. P., Ardis, R., Friesen, P., & Schowen, R. L. (1980a) *J. Am. Chem. Soc. 102*, 5358–5365.

Quinn, D. M., Venkatasubban, K. S., Kise, M., & Schowen, R. L. (1980b) *J. Am. Chem. Soc. 102*, 5365–5369.

Quinn, D. M., Sutton, L. D., & Kinzelman, T. J. (1988) *Am. Biotechnol. Lab. 6*, 33–37.

Rudd, E. A., & Brockman, H. L. (1984) in *Lipases* (Borgström, B., & Brockman, H. L., Eds.) pp 185–204, Elsevier, Amsterdam.

Rudd, E. A., Mizuno, N. K., & Brockman, H. L. (1987) *Biochim. Biophys. Acta 918*, 106–114.

Schowen, K. B. J. (1978) in *Transition States of Biochemical Processes* (Gandour, R. D., & Schowen, R. L., Eds.) pp 225–283, Plenum, New York.

Schowen, K. B., & Schowen, R. L. (1982) *Methods Enzymol. 87*, 551–606.

Schumacher, M., Camp, S., Maulet, Y., Newton, M., MacPhee-Quigley, K., Taylor, S. S., Friedmann, T., & Taylor, P. (1986) *Nature 319*, 407–409.

Stein, R. L., & Strimpler, A. M. (1987) *J. Am. Chem. Soc. 109*, 4387–4390.

Stein, R. L., Strimpler, A. M., Hori, H., & Powers, J. C. (1987) *Biochemistry 26*, 1305–1314.

Stout, J. S., Sutton, L. D., & Quinn, D. M. (1985) *Biochim. Biophys. Acta 837*, 6–12.

Stroud, R. M. (1974) *Sci. Am. 231*, 74–88.

Sutton, L. D., Stout, J. S., Hosie, L., Spencer, P. S., & Quinn, D. M. (1986) *Biochem. Biophys. Res. Commun. 134*, 386–392.

Sutton, L. D., & Quinn, D. M. (1990) *J. Am. Chem. Soc. 112*, 8404–8408.

Sutton, L. D., Stout, J. S., & Quinn, D. M. (1990) *J. Am. Chem. Soc. 112*, 8398–8403.

Tsujita, T., Mizuno, N. K., & Brockman, H. L. (1987) *J. Lipid Res. 28*, 1434–1443.

Verger, R., & DeHaas, G. H. (1976) *Annu. Rev. Biophys. Bioeng. 5*, 77–117.

Wentworth, W. E. (1965) *J. Chem. Educ. 42*, 96–103.